

Kerr black hole parameters and its distance from the Earth in terms of directly measurable quantities of accretion disk

Mehrab Momennia^{1, a}

¹*Instituto de Física y Matemáticas, Universidad Michoacana de San Nicolás de Hidalgo, Edificio C-3, Ciudad Universitaria, CP 58040, Morelia, Michoacán, Mexico.*

(Dated: January 9, 2025)

We extract elegant and concise analytic formulae for the mass and rotation parameters of the Kerr black hole as well as its distance from the Earth only in terms of directly measurable quantities of the accretion disk revolving in the black hole spacetime background. To this end, we consider massive geodesic particles circularly orbiting the Kerr black hole in the equatorial plane and emitting frequency-shifted photons toward a distant observer. We calculate the frequency shift and *redshift rapidity* at the detector location, and by solving an inverse problem, we express the Kerr black hole parameters and its distance from a distant observer in terms of a handful of observable elements, such as frequency shift, aperture angle of the telescope, and *redshift rapidity*, a newly introduced concept in [1]. The aperture angle of the telescope (angular distance) characterizes the emitter position on the sky, and the *redshift rapidity* is an observable relativistic invariant representing the proper time evolution of the frequency shift. The relations presented in this article allow us to disentangle mass, spin, and distance to the black holes in the Kerr spacetime background and obtain these parameters separately. Our analytic formulae are valid on the midline and close to the line of sight, and they can be directly applied to supermassive black holes hosted at the core of active galactic nuclei orbited by water vapor clouds within their accretion disks. The generic exact relations are valid for an arbitrary point of the emitter's orbit, and they can be employed in black hole parameter estimation studies.

Keywords: Kerr black hole, black hole rotation curves, redshift and blueshift, redshift rapidity.

PACS numbers: 11.27.+d, 04.40.-b, 98.62.Gq

I. INTRODUCTION

Even though black holes were first introduced as mathematical solutions to the general theory of relativity in 1915, recent observations of gravitational waves [2] and electromagnetic waves [3, 4] proved their presence in nature. Even before these convincing pieces of evidence, tracking the star trajectories close to the center of the Milky Way galaxy for decades has already provided sufficient data supporting the existence of a supermassive black hole located at the center of our galaxy [5–8] (see [9, 10] for recent results).

On the other hand, an independent general relativistic method for obtaining the black hole parameters has been invented in [11] and further developed in [1, 12, 13] with the aim of utilizing observational frequency shift and *redshift rapidity* detected from massive test particles orbiting black holes. These types of data differ from the ones employed in [2–4]. The initial approach [11] has been introduced based on kinematic redshift/blueshift in order to generalize the similar Keplerian models [14–16] to general relativity.

Lately, by further extending this method, the mass and rotation parameters of the Kerr black hole have been analytically expressed in terms of observational redshift and

blueshift as well as the radius of the emitter that is not an observable quantity [12]. In addition, it was shown that by taking into account the rotating Kerr black hole in a spacetime background with de Sitter asymptote, it is possible to obtain the Hubble (cosmological) constant and black hole parameters with the help of this general relativistic method [13]. Besides, the polymerized black holes have been analyzed and their free parameters were found in terms of the observational frequency shift [17]. Moreover, this method has been developed to generic static and spherically symmetric black hole spacetimes in [18]. This extension allows expressing the free parameters of static black hole spacetimes in modified gravities and general relativity theory coupled to various matter fields in terms of observational frequency shift.

From an observational point of view, there are publicly available observational frequency shift data from supermassive black holes hosted at the core of the active galactic nuclei (AGNs) (see [14–16] for instance). In these astrophysical systems, water vapor clouds are circularly orbiting the central black hole within the accretion disk and water molecules emit frequency-shifted photons toward a far away detector. In these specific systems, the total frequency shift and aperture angle of the telescope are the observational quantities, and therefore, one can employ this general relativistic approach to estimate the Mass-to-Distance (M/D) ratio of the central black hole. Following this capability, the mass-to-distance ratio of several supermassive Schwarzschild black holes hosted at the core of AGNs has been estimated in [19–23].

^aElectronic address: momennia1988@gmail.com

It is worthwhile to mention that although the gravitational redshift produced by the central compact object has been quantified in the M/D estimations performed in [19–23], the mass-to-distance ratio of the central supermassive Schwarzschild black hole has been estimated only. This is because the mass-to-distance ratio is degenerate in this general relativistic formalism and one has to use another observational element to break the M/D degeneracy. In order to resolve this issue, we have introduced a new general relativistic invariant observable parameter called the *redshift rapidity* that describes the evolution of the frequency shift with respect to the proper time [1]. As a result, the M/D degeneracy in the Schwarzschild spacetime background has been broken with the help of the *redshift rapidity*, and consequently, the mass of the Schwarzschild black hole and its distance from the Earth have been expressed fully in terms of directly observational quantities through concise and elegant analytic formulae.

A similar degeneracy is also present for the mass-to-distance ratio and charge-to-distance ratio in the Reissner-Nordström black hole spacetime. Therefore, the *redshift rapidity* has been computed in the Reissner-Nordström background and it has been used to break these degeneracies in order to extract analytic formulae for the mass of the Reissner-Nordström black hole, its electric charge, and its distance from a distant observer in terms of directly observational elements [24]. The obtained relations for the Schwarzschild and Reissner-Nordström black hole solutions could help to measure the distance to these black holes and compute their parameters. The initial aim of introducing the redshift rapidity was to improve the precision in measuring cosmic distances with respect to the previous attempts based on post-Newtonian methods that measure the angular-diameter distance to galaxies [16, 25–27]. In this study, we compute the *redshift rapidity* in the Kerr background, and with the aid of the total frequency shifts, we obtain concise and elegant analytic formulae for the black hole mass, its spin, and its distance from a distant observer fully in terms of directly observational quantities. The complete expressions of the frequency shift and *redshift rapidity* as well as the analytic formulae could enable one to obtain the Kerr black hole mass, spin, and its distance from the Earth.

The outline of this paper is as follows. The first part of the next section is devoted to a review of the general relativistic method and the frequency shift of massive geodesic particles circularly orbiting the Kerr black hole in the equatorial plane. Then, we express the mass-to-distance ratio and the spin-to-distance ratio of the Kerr black hole in terms of observable frequency shifts on the midline and close to the line of sight (LOS). In Sec. III, we define *redshift rapidity* in the Kerr background as the derivative of the frequency shift with respect to the proper time. Then, we obtain the *redshift rapidity* on the midline and close to the LOS, and with the aid of the corresponding mass-to-distance ratio and spin-to-

distance ratio, we express the mass and spin of the black hole and its distance from the Earth in terms of direct observational quantities. Finally, we finish our paper with some concluding remarks in Sec. IV.

II. FREQUENCY SHIFT IN KERR BACKGROUND

In this section, we first briefly review previous results from a general relativistic method to obtain the frequency shift formulae of massive probe particles revolving in Kerr spacetime background based on [12], and then describe our original contribution. We first consider the geodesic motion of massive test particles orbiting a Kerr black hole which emit photons toward a distant observer. We present a formula for the redshift of the detected photons coming from a general point of their orbit in the equatorial plane which depends on the azimuthal angle φ . Then, we obtain the mass-to-distance ratio and spin-to-distance ratio of the Kerr black hole in terms of directly measurable elements for two special points on the midline $\varphi \approx \pi/2$ and close to the LOS $\varphi \approx 0$.

The spacetime background of the Kerr black hole is described by the line element

$$ds^2 = g_{tt}dt^2 + 2g_{t\varphi}dtd\varphi + g_{\varphi\varphi}d\varphi^2 + g_{rr}dr^2 + g_{\theta\theta}d\theta^2, \quad (1)$$

with the metric components

$$g_{tt} = -\left(1 - \frac{2Mr}{\Sigma}\right), \quad g_{t\varphi} = -\frac{2Mar \sin^2 \theta}{\Sigma}, \quad g_{rr} = \frac{\Sigma}{\Delta},$$

$$g_{\varphi\varphi} = \left(r^2 + a^2 + \frac{2Ma^2r \sin^2 \theta}{\Sigma}\right) \sin^2 \theta, \quad g_{\theta\theta} = \Sigma,$$

$$\Delta = r^2 + a^2 - 2Mr, \quad \Sigma = r^2 + a^2 \cos^2 \theta,$$

where M is the total mass of the Kerr black hole and a is its total angular momentum per unit mass, $a = J/M$ ($0 \leq a \leq M$). The Kerr spacetime has an intrinsic ring singularity of radius a in the equatorial plane, whereas its Cauchy horizon r_- and event horizon r_+ surfaces are located at

$$r_{\pm} = M \pm \sqrt{M^2 - a^2}. \quad (2)$$

In axially symmetric spacetimes of the form (1), the frequency shift of photons emitted by massive geodesic particles orbiting the black hole and detected by an observer is given by [11]

$$1 + z_{\text{Kerr}} = \frac{\omega_e}{\omega_d} = \frac{(E_{\gamma}U^t - L_{\gamma}U^{\varphi} - g_{rr}U^r k^r - g_{\theta\theta}U^{\theta} k^{\theta})|_e}{(E_{\gamma}U^t - L_{\gamma}U^{\varphi} - g_{rr}U^r k^r - g_{\theta\theta}U^{\theta} k^{\theta})|_d}, \quad (3)$$

where $\omega_p = -(k_\mu U^\mu)|_p$ is the frequency of a photon emitted (detected) by an emitter (detector) at the emission (detection) point p , k_p^μ is the 4-wave vector of the photon, and U_p^μ is the proper 4-velocity of the emitter (observer). Besides, E_γ and L_γ are conserved along the light trajectories and correspond to the total energy and axial angular momentum of the photons, respectively. The relation (3) holds for the frequency shift of arbitrary stable orbits of the test massive particles, such as circular, elliptic, non-equatorial, etc.

Now, because of the existing data regarding the accretion disks as well as being able to extract analytic formulae for mass, spin, and distance to the Kerr black hole, we restrict ourselves to the circular motion of the photon sources ($U_e^r = 0$) which is the case for real astrophysical systems containing the accretion disks [19, 28]. In addition, we put both the emitter and observer in the equatorial plane ($\theta = \pi/2$), for which we have $U_e^\theta = 0 = U_d^\theta$, due to the fact that any tilted disk should be driven to the equatorial plane of the rotating spacetime backgrounds [29] ($U_e^\theta = 0$) and accretion disks can be detected mostly in an edge-on view from the Earth [28, 30] ($U_d^\theta = 0$). In the special case of a distant observer $r_d \rightarrow \infty$ (which is the case for the real astrophysical systems in AGNs), the 4-velocity of the detector simplifies to $U_d^\mu = \delta_t^\mu$. By taking into account these assumptions, the generic relation (3) reduces to

$$1 + z_{Kerr} = \frac{(E_\gamma U^t - L_\gamma U^\varphi)|_e}{(E_\gamma U^t)|_d} = U_e^t - b_\varphi U_e^\varphi, \quad (4)$$

where $b_\varphi \equiv L_\gamma/E_\gamma$ is the deflection of light parameter which gives the light bending produced by the gravitational field of the Kerr black hole. The nonvanishing components of the 4-velocity U_e^μ are given by [12]

$$U_e^t(r_e, \pi/2) = \frac{r_e^{3/2} \pm aM^{1/2}}{r_e^{3/4} \sqrt{r_e^{3/2} - 3Mr_e^{1/2} \pm 2aM^{1/2}}}, \quad (5)$$

with $\tilde{M} = M/r_e$, $\tilde{a} = a/r_e$, and $\tilde{\Delta}_e = \Delta_e/r_e^2 = 1 + \tilde{a}^2 - 2\tilde{M}$. In this relation, the upper sign corresponds to the co-rotating photon courses and the lower sign corresponds to the counter-rotating ones. In what follows we shall restrict ourselves to the co-rotating emitters since the case of counter-rotating ones is quite similar and one only needs following the same steps as we discuss here for the co-rotating particles.

Besides, the innermost stable circular orbit (ISCO) ra-

$$U_e^\varphi(r_e, \pi/2) = \pm \frac{M^{1/2}}{r_e^{3/4} \sqrt{r_e^{3/2} - 3Mr_e^{1/2} \pm 2aM^{1/2}}}, \quad (6)$$

where r_e is the radius of the emitter, the upper sign refers to a co-rotating emitter (the angular momentum of the massive test particle is in the same direction as the Kerr black hole), and the lower sign corresponds to a counter-rotating one. Also, one can calculate the $(\varphi + \delta)$ -dependent light bending parameter b_φ for an arbitrary point of the circular orbit of photon sources on the equatorial plane which is presented in Eq. (A.11) of the appendix, and for the Kerr black hole case, converts to [see also Fig. 2 for the geometrical illustration of the azimuthal angle φ and the angular distance δ , and their relation]

$$b_\varphi = -\frac{2aM}{r_e - 2M} + \frac{r_e \Delta_e^{3/2} \sin(\varphi + \delta)}{(r_e - 2M)} \times \frac{1}{\sqrt{\Delta_e^2 \sin^2(\varphi + \delta) + (r_e - 2M) r_e^3 \cos^2(\varphi + \delta)}} \quad (7)$$

where $\Delta_e = \Delta|_{r=r_e}$, φ is the azimuthal angle that is not a measurable quantity, and δ is the aperture angle of the telescope (angular distance) that is an observable parameter. It is worth mentioning that because of the dragging effect produced by the rotation nature of the Kerr black hole, b_φ does not vanish at the line of sight where $\varphi = 0 = \delta$, in contrast to the Schwarzschild case. In addition, the observable δ is a function of the azimuthal angle φ for an arbitrary point on the circular orbit through Eq. (A.15) (see Fig. 2 of the appendix and related discussion).

Now, by substituting (5)-(7) into (4), we obtain the following explicit form of the frequency shift for an arbitrary point of the orbit on the equatorial plane

$$1 + z_{Kerr} = \frac{1}{(1 - 2\tilde{M}) \sqrt{1 - 3\tilde{M} \pm 2\tilde{a} \tilde{M}^{1/2}}} \left[1 - 2\tilde{M} \pm \tilde{M}^{1/2} \left(\tilde{a} + \frac{\tilde{\Delta}_e^{3/2} \sin(\varphi + \delta)}{\sqrt{\tilde{\Delta}_e^2 \sin^2(\varphi + \delta) + (1 - 2\tilde{M}) \cos^2(\varphi + \delta)}} \right) \right], \quad (8)$$

dus in the Kerr spacetime reads [31]

$$r_{ISCO} = M \left(3 + \beta \mp \sqrt{(3 - \alpha)(3 + \alpha + 2\beta)} \right), \quad (9)$$

$$\alpha = 1 + \left(1 - \frac{a^2}{M^2} \right)^{1/3} \left[\left(1 + \frac{a}{M} \right)^{1/3} + \left(1 - \frac{a}{M} \right)^{1/3} \right],$$

$$\beta = \sqrt{\alpha^2 + 3 \frac{a^2}{M^2}},$$

that approximately characterizes the inner edge of the accretion disk. In this article, we are interested in stable circular orbits of the photon sources such that $r_e \geq r_{ISCO}$, and this restriction on the emitter radius leads to an upper bound on the frequency shift of the emitted photons (see the dashed curves in Fig. 2 of [12]).

Figure 1 illustrates the general behavior of the redshift formula (8) versus the azimuthal angle φ for the co-rotating massive test particles. This figure indicates how the frequency shift in the Kerr background modifies with the motion of the geodesic particle and how it changes for non-zero values of the rotation parameter. The non-vanishing value of the redshift at the LOS ($\varphi = 0$) for the continuous green curve (referring to the standard Schwarzschild black hole) quantifies the magnitude of the gravitational redshift. The difference between the other curves and the green one is due to the dragging effect produced by the rotation nature of the Kerr black hole. Furthermore, the total frequency shift is maximal close to the midline ($\varphi \approx \pm\pi/2$), and therefore, it is easier to be measured observationally.

On the other hand, one may note that in the Newtonian limit $\tilde{M}, \tilde{a} \rightarrow 0$, the redshift formula of the Kerr black hole z_{Kerr} presented in Eq. (8) reduces to

$$z_{Newton} = \tilde{M}^{1/2} \sin(\varphi + \delta) + \mathcal{O}(\tilde{M}), \quad (10)$$

which is the projection of the Keplerian velocity of a circularly orbiting particle on the LOS, as it should be.

As the next step, we are going to express the mass-to-distance ratio M/D and spin-to-distance ratio a/D of the Kerr black hole in terms of directly measurable quantities for two special important cases of the midline $\varphi \approx \pi/2$ and close to the LOS $\varphi \approx 0$. These two cases have significant importance due to the fact that they describe the frequency shift of emitters within accretion disks circularly orbiting supermassive black holes hosted at the core of AGNs and there are available astrophysical data from these specific points.

A. Frequency shift on the midline

When the position vector of orbiting objects with respect to the black hole location is approximately orthogonal to the observer's LOS ($k^r = 0$), we can measure the high frequency shifted photons on the midline where $\varphi = \pm\pi/2$. Therefore, for the highly redshifted ($\varphi = +\pi/2$) and blueshifted ($\varphi = -\pi/2$) photons, the frequency shift formula (8) reduces to

$$1 + z_{Kerr1,2}^{(m)} \approx \frac{(1 - 2\tilde{M}) + \tilde{M}^{1/2} (\tilde{a} \pm \tilde{\Delta}_e^{1/2})}{(1 - 2\tilde{M}) \sqrt{1 - 3\tilde{M} + 2\tilde{a}\tilde{M}^{1/2}}}, \quad (11)$$

in the limit $\delta \rightarrow 0$ that is the case for the real astrophysical systems where the angular distance is of the order

of milliarcseconds. Here and in what follows, the index “ m ” means the observational quantities should be measured on the midline. This relation is obtained for the co-rotating photon sources and the plus (minus) sign refers to the redshifted (blueshifted) photons denoted by $z_{Kerr1}^{(m)}$ ($z_{Kerr2}^{(m)}$) on the midline. By multiplying $R_m := 1 + z_{Kerr1}^{(m)}$ and $B_m := 1 + z_{Kerr2}^{(m)}$, one can find the mass-to-distance ratio and spin-to-distance ratio of the Kerr black hole in terms of directly observational elements on the midline as follows [12]

$$\frac{M}{D} = \frac{R_m B_m - 1}{2R_m B_m} \delta_m := \mathcal{M}(R_m, B_m) \delta_m, \quad (12)$$

$$\frac{a}{D} = \frac{\delta_m}{(2R_m B_m)^{3/2} \sqrt{R_m B_m - 1}} \times \left[(R_m - B_m)^2 - (R_m + B_m) \sqrt{R_m^2 + B_m^2 - 2R_m^2 B_m^2} \right] := \mathcal{A}(R_m, B_m) \delta_m, \quad (13)$$

up to the first order in δ_m in consistency with the condition $U_d^\mu = \delta_t^\mu$ for distant observers. In order to derive the aforementioned relations, we also employed the approximation $r_e \approx D\delta_m$ given in Eq. (A.13) where the observable δ_m should be measured on the midline. Equations (12)-(13) show that M/D and a/D of the Kerr black hole are expressed in terms of directly measurable quantities $\{R_m, B_m, \delta_m\}$, but they are degenerate and we shall disentangle them in the upcoming section.

B. Frequency shift close to the line of sight

Calculating the frequency shift of emitters in the vicinity of the LOS of their orbital motion is also important for astrophysical applications. Therefore, for angles close to zero on either side of the LOS where $\varphi_s \rightarrow 0$ and $\delta_s \rightarrow 0$, one finds the frequency shift formula (8) reduces to

$$1 + z_{Kerr1,2}^{(s)} \approx \frac{(1 - 2\tilde{M}) + \tilde{M}^{1/2} \left[\tilde{a} \pm (1 - 2\tilde{M})^{-1/2} \tilde{\Delta}_e^{3/2} (\varphi_s + \delta_s) \right]}{(1 - 2\tilde{M}) \sqrt{1 - 3\tilde{M} + 2\tilde{a}\tilde{M}^{1/2}}}, \quad (14)$$

for the slightly redshifted $z_{Kerr1}^{(s)}$ and slightly blueshifted $z_{Kerr2}^{(s)}$ photons. Here and in what follows, the index “ s ” corresponds to the measurements close to the LOS. $z_{Kerr1,2}^{(s)}$ are obtained for the co-rotating particles only, and the angles δ_s and φ_s should be measured close to the LOS. Note that δ_s is an observable parameter whereas φ_s is not, and they are related to each other through the approximation (A.14). The relations (14) reduce to the gravitational redshift $z_g = z_{Kerr1}^{(s)} = z_{Kerr2}^{(s)}$ exactly at the LOS where $\varphi_s = 0 = \delta_s$, and interestingly, one can quantify the dragging effect at this point explicitly.

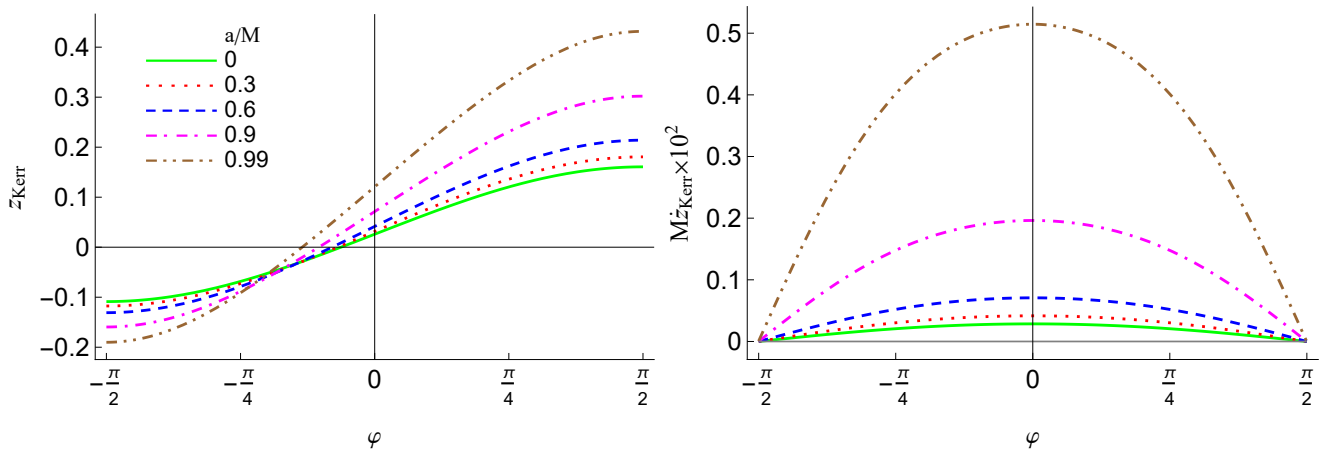


FIG. 1: The frequency shift z_{Kerr} (left panel) and the *redshift rapidity* \dot{z}_{Kerr} (right panel) versus the azimuthal angle φ in the Kerr black hole spacetime for $r_e = 10r_{ISCO}$, $D = 10^4 r_{ISCO}$, and different values of the rotation parameter. The continuous green curves correspond to the Schwarzschild black hole, and the difference between the other curves and the green one is due to the dragging effect. The redshift and blueshift are maximal on the midline where $\varphi \approx \pm\pi/2$ while we see that the *redshift rapidity* is maximum close to the line of sight where $\varphi \approx 0 \approx \delta$. In order to plot these curves, we substituted δ given in Eq. (A.15) into the frequency shift formula (8) and the *redshift rapidity* formula (19).

Unlike the midline case, one finds that $z_{Kerr_{1,2}}^{(s)}$ are rather complicated to find M/D and a/D in terms of observables $\{z_{Kerr_1}^{(s)}, z_{Kerr_2}^{(s)}, \delta_s\}$. On the other hand, since R_m and B_m of the midline case are easier to be measured observationally, it is important to incorporate them in the LOS case where the *redshift rapidity* is maximal (see the next section and the right panel of Fig. 1). Therefore, by noting that $\tilde{M} = M/r_e$, we substitute $\tilde{M} = M/(D\delta_m) = \mathcal{M}(R_m, B_m)$ from Eq. (12) into (14) and solve $(1 + z_{Kerr_1}^{(s)}) + (1 + z_{Kerr_2}^{(s)})$ to obtain

$$\frac{a\varphi_s}{D\delta_s} = \frac{(1-2\mathcal{M})}{\sqrt{\mathcal{M}}} \left[-1 + \left(\frac{R_s + B_s}{2} \right)^2 \times \left((1-2\mathcal{M}) - \sqrt{(1-2\mathcal{M})^2 - \frac{4(1-\mathcal{M})}{(R_s + B_s)^2}} \right) \right] \\ := \mathcal{F}(R_m, B_m, R_s, B_s), \quad (15)$$

for the spin-to-distance ratio of the Kerr black hole close to the LOS that is a function of a set of purely measurable elements $\{R_s, B_s, R_m, B_m\}$ with $R_s := 1 + z_{Kerr_1}^{(s)}$ and $B_s := 1 + z_{Kerr_2}^{(s)}$. To derive this relation, we applied the limits $\delta_s, \varphi_s \rightarrow 0$ and employed the approximation $r_e \approx D\delta_s/\varphi_s$ from Eq. (A.14) valid close to the LOS. One may note that the unobservable parameter φ_s can be expressed in terms of the set of purely observational quantities $\{R_s, B_s, \delta_s; R_m, B_m, \delta_m\}$ by substituting a/D from (13) into (15).

III. REDSHIFT RAPIDITY IN KERR BACKGROUND

The mass-to-distance ratio (12) in the static limit $a \rightarrow 0$ reduces to the corresponding one in the standard Schwarzschild spacetime. So far this relation has been employed to estimate the mass-to-distance ratio of several supermassive Schwarzschild black holes hosted at the center of galaxies [19–23]. However, note that the mass-to-distance ratio (12) as well as spin-to-distance ratios (13) and (15) are degenerate. In order to disentangle the mass M and spin a of the Kerr black hole as well as its distance from the Earth D and express them through closed formulae in terms of observational quantities, we employ the *redshift rapidity*, a new concept introduced in the standard Schwarzschild spacetime recently in [1]. In a similar manner to [1], one can define the *redshift rapidity* in the Kerr spacetime background at the emission point as the proper time evolution of the frequency shift z_{Kerr} (4) in the following way

$$\dot{z}_{Kerr}|_{r=r_e} = \frac{dz_{Kerr}}{d\tau} = \frac{d}{d\tau}(U_e^t - b_\varphi U_e^\varphi), \quad (16)$$

where τ is the proper time. Since the observer measures the *redshift rapidity* here on the Earth, we rewrite Eq. (16) at the detector position as

$$\dot{z}_{Kerr} = \frac{dz_{Kerr}}{dt} = \frac{d\tau}{dt} \frac{dz_{Kerr}}{d\tau} = \frac{1}{U_e^t} \frac{d}{d\tau}(U_e^t - b_\varphi U_e^\varphi), \quad (17)$$

in which we used $U_e^t = \frac{dt}{d\tau}|_{r=r_e}$, and \dot{z}_{Kerr} is an observable quantity now. For the photon sources circularly orbiting the Kerr black hole in the equatorial plane, U_e^t (5) and U_e^φ (6) of the 4-velocity are constant, whereas the light bending parameter (7) is time-dependent through

δ and φ . Therefore, the *redshift rapidity* relation (17) reduces to

$$\dot{z}_{Kerr} = -\frac{db_\varphi}{d\tau} \frac{U_e^\varphi}{U_e^t} = -\left(\frac{\partial b_\varphi}{\partial \varphi} + \frac{\partial b_\varphi}{\partial \delta} \frac{\partial \delta}{\partial \varphi}\right) \frac{(U_e^\varphi)^2}{U_e^t}, \quad (18)$$

where we used $U_e^\varphi = \frac{d\varphi}{d\tau}\Big|_{r=r_e}$ in the last step and note that δ is related to φ through Eq. (A.15).

By considering the light bending parameter (7) and the δ function (A.15), one can perform the aforementioned derivatives to find the *redshift rapidity* in the Kerr background for an arbitrary point on the circular motion as follows

$$\dot{z}_{Kerr} = \frac{DMr_e^4 \Delta_e^{3/2} (D - r_e \cos \varphi) \cos(\varphi + \delta)}{\left[r_e^4 \left(1 - \frac{2M}{r_e}\right) \cos^2(\varphi + \delta) + \Delta_e^2 \sin^2(\varphi + \delta)\right]^{\frac{3}{2}}} \times \frac{(D^2 + r_e^2 - 2Dr_e \cos \varphi)^{-1}}{(r_e^2 + a\sqrt{Mr_e}) \sqrt{r_e^2 + 2a(Mr_e)^{\frac{1}{2}} - 3Mr_e}}, \quad (19)$$

which reduces to the *redshift rapidity* in the Schwarzschild spacetime background in the limit $a \rightarrow 0$ [1].

The profile of the *redshift rapidity* versus the azimuthal angle φ in the Kerr background is illustrated in Fig. 1 for various values of the rotation parameter. This figure shows that \dot{z}_{Kerr} is maximal at the LOS, and therefore it is easier to be measured for small angles $\varphi \approx 0$. One can also see that the *redshift rapidity* increases as the rotation parameter increases.

Interestingly, in the Newtonian limit $M/r_e \rightarrow 0$ and $a/r_e \rightarrow 0$, the *redshift rapidity* formula (19) reduces to the projection of the Keplerian acceleration of a circularly orbiting massive test particle on the LOS

$$\dot{z}_{Newton} = \frac{M}{r_e^2} \cos(\varphi + \delta) + \mathcal{O}\left(\frac{M^2}{r_e^3}\right), \quad (20)$$

for large distances $r_e/D \rightarrow 0$, as we expected.

Now, one can use the *redshift rapidity* formula in Kerr spacetime (19) as well as M/D and a/D given in Eqs. (12)-(13) on the midline to disentangle the Kerr black hole mass M , its rotation parameter a , and its distance from Earth D , thus obtaining analytic relations for these parameters at these specific points. On the other hand, we can employ Eq. (19) and a/D on the LOS given in Eq. (15) in order to find an analytic formula for the distance to Kerr black holes in terms of the frequency shift on the midline and the *redshift rapidity* close to the LOS.

In what follows, we analyze two important cases of the midline and close to the LOS describing water vapor clouds within accretion disks circularly orbiting supermassive black holes hosted at the center of AGNs for which data is available for frequency shift and *redshift rapidity*.

A. *Redshift rapidity on the midline*

The emitted photons on the midline are highly redshifted/blueshifted whereas they have low *redshift rapidity*. The mass-to-distance ratio and spin-to-distance ratio of the central Kerr black hole are presented through Eqs. (12)-(13) in terms of observational redshifted/blueshifted detected photons and the angular distance of their source. On the other hand, by setting $\varphi = \varphi_m = \pi/2$ as well as introducing the approximations (A.13) and $\delta_m \rightarrow 0$ in the *redshift rapidity* formula (19), one can obtain $\dot{z}_{Kerr}^{(m)}$ corresponding to the same redshifted/blueshifted photons on the midline as follows

$$\dot{z}_{Kerr}^{(m)} \approx \frac{\frac{M}{D\delta_m}}{D \left(\frac{a}{D\delta_m} \sqrt{\frac{M}{D\delta_m}} + 1\right)} \times \frac{1}{\left[\left(\frac{a}{D\delta_m}\right)^2 - 2\frac{M}{D\delta_m} + 1\right]^{\frac{3}{2}} \sqrt{2\frac{a}{D\delta_m} \left(\frac{M}{D\delta_m}\right)^{\frac{1}{2}} - 3\frac{M}{D\delta_m} + 1}}. \quad (21)$$

As the final step, we solve Eqs. (12)-(13) and (21) to find the mass of the Kerr black hole, its rotation parameter, and its distance from the Earth as below

$$M = \frac{\mathcal{M}^2 \mathcal{X}}{\dot{z}_{Kerr}^{(m)} \left(\mathcal{A}\sqrt{\mathcal{M}} + 1\right)} \delta_m, \quad (22)$$

$$a = \frac{\mathcal{A}\mathcal{M}\mathcal{X}}{\dot{z}_{Kerr}^{(m)} \left(\mathcal{A}\sqrt{\mathcal{M}} + 1\right)} \delta_m, \quad (23)$$

$$D = \frac{\mathcal{M}\mathcal{X}}{\dot{z}_{Kerr}^{(m)} \left(\mathcal{A}\sqrt{\mathcal{M}} + 1\right)}, \quad (24)$$

$$\mathcal{X} = \frac{1}{\sqrt{2\mathcal{A}\mathcal{M}^{1/2} - 3\mathcal{M} + 1} (\mathcal{A}^2 - 2\mathcal{M} + 1)^{3/2}}, \quad (25)$$

in terms of the set of fully observational quantities $\left\{z_{Kerr_1}^{(m)}, z_{Kerr_2}^{(m)}, \dot{z}_{Kerr}^{(m)}, \delta_m\right\}$ that should be measured on the midline. One can also obtain the radius of the emitter, which is not an observational element, with the help of Eqs. (24) and (A.13) as

$$r_e = \frac{\mathcal{M}\mathcal{X}}{\dot{z}_{Kerr}^{(m)} \left(\mathcal{A}\sqrt{\mathcal{M}} + 1\right)} \delta_m. \quad (26)$$

Now, it would be helpful to find an analytic relation for the distance D in terms of observations close to the LOS since the *redshift rapidity* is maximal at this point and easier to be measured. In addition, it would be nice to have this distance in terms of redshift and blueshift on the midline as well where these quantities are maximal. We shall obtain such a distance to the Kerr black hole in the next subsection.

B. Redshift rapidity close to the line of sight

Here we take into account the slightly frequency-shifted emitters close to the LOS with maximal *redshift rapidity* and the spin-to-distance ratio of the corresponding Kerr black hole is presented in Eq. (15) in terms of the redshift/blueshift for $\varphi_s \approx 0$. First, from the ap-

proximation (A.14), we see that $r_e = aD\delta_s/(a\varphi_s)$ where $a\varphi_s/(D\delta_s)$ is given in terms of observations in Eq. (15). Hence, we replace r_e with the aforementioned relation in the *redshift rapidity* formula (19). Next, by keeping the term $a\varphi_s/(D\delta_s)$, we divide the rest of M and a parameters by $D\delta_m$ to get

$$\dot{z}_{Kerr}^{(s)} \approx \frac{\left(\frac{a\varphi_s}{D\delta_s}\right)^3 \left(\frac{M}{D\delta_m}\right) \left[\left(\frac{a\varphi_s}{D\delta_s}\right)^2 \left(\frac{a}{D\delta_m}\right) - 2 \left(\frac{a\varphi_s}{D\delta_s}\right) \left(\frac{M}{D\delta_m}\right) + \frac{a}{D\delta_m} \right]^{3/2}}{D \left(\frac{a}{D\delta_m}\right) \delta_m \left[\frac{a\varphi_s}{D\delta_s} - \left(\frac{a}{D\delta_m}\right) \delta_m \right] \left[\left(\frac{a\varphi_s}{D\delta_s}\right)^{3/2} \sqrt{\frac{M}{D\delta_m} + \sqrt{\frac{a}{D\delta_m}}} \left[\frac{a}{D\delta_m} - 2 \left(\frac{a\varphi_s}{D\delta_s}\right) \left(\frac{M}{D\delta_m}\right) \right]^{3/2}} \right]} \times \frac{1}{\sqrt{2 \left(\frac{a\varphi_s}{D\delta_s}\right)^{3/2} \left(\frac{a}{D\delta_m}\right)^{1/2} \left(\frac{M}{D\delta_m}\right)^{1/2} - 3 \left(\frac{a\varphi_s}{D\delta_s}\right) \left(\frac{M}{D\delta_m}\right) + \frac{a}{D\delta_m}}}, \quad (27)$$

for the *redshift rapidity* of photon sources close to the LOS and we applied the limits $\delta_s, \varphi_s \rightarrow 0$ as well. Finally, we substitute Eqs. (12)-(13) and (15) into (27) and solve the resultant relation for D to obtain the distance as

$$D = \frac{\mathcal{F}^3 \mathcal{M} (\mathcal{A}\mathcal{F}^2 + \mathcal{A} - 2\mathcal{F}\mathcal{M})^{3/2}}{\dot{z}_{Kerr}^{(s)} \mathcal{A} \delta_m \sqrt{\mathcal{A} - 3\mathcal{F}\mathcal{M} + 2\mathcal{F}(\mathcal{A}\mathcal{F}\mathcal{M})^{1/2}}} \times \frac{1}{(\mathcal{F} - \mathcal{A}\delta_m)(\mathcal{A} - 2\mathcal{F}\mathcal{M})^{3/2} \left(\sqrt{\mathcal{A}} + \mathcal{F}\sqrt{\mathcal{F}\mathcal{M}}\right)}, \quad (28)$$

fully in terms of the set of observational quantities $\left\{ z_{Kerr_1}^{(s)}, z_{Kerr_2}^{(s)}, \dot{z}_{Kerr}^{(s)}, z_{Kerr_1}^{(m)}, z_{Kerr_2}^{(m)}, \delta_m \right\}$ where $\left\{ z_{Kerr_1}^{(s)}, z_{Kerr_2}^{(s)}, \dot{z}_{Kerr}^{(s)} \right\}$ should be measured close to the LOS and $\left\{ z_{Kerr_1}^{(m)}, z_{Kerr_2}^{(m)}, \delta_m \right\}$ should be measured on the midline. From an observational point of view, this is a significant formula for the Kerr black hole distance from the Earth since it is a combination of highly redshifted photons on the midline and maximum *redshift rapidity* on the LOS, and therefore, they are easier to be measured.

As the final remark, we would like to stress that the analytic formulae for the Kerr black hole mass M (22), its rotation parameter a (23), and its distance from the Earth D (24) & (28) are presented fully in terms of directly measurable quantities of the accretion disk, and they are among the crucial findings of the present study. In addition, the complete forms of the frequency shift relation (8) and *redshift rapidity* formula (19) can be employed in black hole parameter estimation studies for an arbitrary point on the circular motion of the emitter in order to obtain M , a , and D of Kerr black holes. For instance, the general expressions (8) and (19) can find astrophysical applications for modeling the accretion disks consisting of water masers revolving supermassive black

holes hosted at the core of AGNs (see [19–23] for the Schwarzschild black hole modelings).

IV. DISCUSSION AND FINAL REMARKS

In this paper, we have considered the frequency shift of photon sources circularly orbiting a Kerr black hole in the equatorial plane for an arbitrary point on the circular motion of the orbiting particles by taking into account the non-zero angular distance. Then for a special case on the midline, we represented the mass-to-distance ratio and spin-to-distance ratio of the Kerr black hole only in terms of observable quantities, that have been already obtained in [12]. Besides, we have calculated the spin-to-distance ratio of the Kerr black hole close to the LOS in terms of observational elements. On the other hand, we have computed the proper time evolution of the frequency shift in order to calculate the *redshift rapidity* in the Kerr spacetime background. Then, we employed the *redshift rapidity* on the midline to express the Kerr black hole mass and spin as well as its distance from the Earth fully in terms of directly measurable quantities. In this scenario, the *redshift rapidity* is a general relativistic invariant observational parameter as well that is calculated as the derivative of the frequency shift with respect to the proper time in the Kerr black hole spacetime. In addition, we employed the *redshift rapidity* close to the LOS as well as the mass-to-distance ratio and spin-to-distance ratio on the midline in order to obtain the distance to the Kerr black hole. This distance formula is significantly important from an observational point of view since it is a function of highly redshifted photons on the midline and maximum *redshift rapidity* on the LOS, i.e., the quantities that are easier to be measured.

We have derived concise and elegant analytic formulae

on the midline and close to the LOS that allow us to disentangle the mass and spin of the Kerr black hole as well as its distance from a distant observer, hence being able to estimate these parameters separately. Our analytic formulae are valid on the midline and close to the line of sight, having direct application to supermassive black holes hosted at the core of active galactic nuclei orbited by water vapor clouds within their accretion disks. The generic exact expressions are valid for an arbitrary point of the emitter's orbit, and they can be employed in black hole parameter estimation studies.

Indeed, one can apply the generic exact relations to real astrophysical systems where water maser clouds are circularly orbiting a central supermassive black hole in the equatorial plane [28, 32, 33], as was accomplished in the Schwarzschild black hole case [19–23]. As a concrete example, we refer to supermassive black holes hosted at the core of the galaxies NGC 4258 and NGC 2273 where their accretion disks made of water masers circularly orbiting the central object in the equatorial plane, and such megamaser systems have been tracked for several galaxies using astrometry techniques. On the other hand, the analytic formulae on the midline and close to the LOS can be applied to the photon sources located at these special positions where can be detected for most megamaser systems (see [28, 32] for instance).

Acknowledgements

The author is grateful to A. Herrera-Aguilar and U. Nucamendi for carefully reading the manuscript. He also acknowledges SNII and was supported by the National Council of Humanities, Sciences, and Technologies of Mexico (CONAHCyT) through Estancias Posdoctorales por México Convocatoria 2023(1) under the postdoctoral Grant No. 1242413.

Appendix: $(\varphi + \delta)$ -dependent light bending parameter in Kerr spacetime

In this appendix, we combine section V of [12] and the appendix of [1] to obtain the light bending parameter of the photon sources for an arbitrary point on their circular orbit in the equatorial plane mainly for the self-consistency of the article. Indeed, the angular distance δ has been neglected in [12] due to the fact that the black holes are located far from the Earth. But even though δ is small, its dependency on time is important in the derivation of the *redshift rapidity* formula, hence we take into account its contribution to the light bending parameter in this article.

Fig. 2 shows that the frequency-shifted photons can arrive at the detector from any generic point on their circular motion in the equatorial plane. The light bending parameter of such generic photons in the axially symmetric spacetime backgrounds of the form (1) can be

calculated from the equation of motion of null particles ($g_{\mu\nu}k^\mu k^\nu = 0$) laying in the equatorial plane as

$$g_{tt}(k^t)^2 + g_{rr}(k^r)^2 + 2g_{t\varphi}k^t k^\varphi + g_{\varphi\varphi}(k^\varphi)^2 = 0, \quad (\text{A.1})$$

where k^t and k^φ can be written in terms of the constants of motions E_γ and L_γ with the help of the temporal Killing vector field $\xi^\mu = \delta_t^\mu$ and the rotational Killing vector field $\psi^\mu = \delta_\varphi^\mu$ as follows

$$k^t = \frac{E_\gamma g_{\varphi\varphi} + L_\gamma g_{t\varphi}}{g_{t\varphi}^2 - g_{tt}g_{\varphi\varphi}}, \quad (\text{A.2})$$

$$k^\varphi = -\frac{E_\gamma g_{t\varphi} + L_\gamma g_{tt}}{g_{t\varphi}^2 - g_{tt}g_{\varphi\varphi}}. \quad (\text{A.3})$$

By substituting Eqs. (A.2)-(A.3) into the equation of motion (A.1), one finds k^r in terms of the metric components and constants of motion in the following form

$$(k^r)^2 = \frac{g_{tt}L_\gamma^2 + 2g_{t\varphi}L_\gamma E_\gamma + g_{\varphi\varphi}E_\gamma^2}{g_{rr}(g_{t\varphi}^2 - g_{tt}g_{\varphi\varphi})}. \quad (\text{A.4})$$

As illustrated in Fig. 2, we define the auxiliary bidimensional vector K with the decomposition

$$k^r = K \cos \alpha, \quad (\text{A.5})$$

$$r_e k^\varphi = K \sin \alpha, \quad (\text{A.6})$$

with

$$K^2 = (k^r)^2 + r_e^2 (k^\varphi)^2. \quad (\text{A.7})$$

where the angular distance is non-zero and the angle $\alpha = \varphi + \delta$ specifies the propagation direction K of the photons and the radial component of the 4-wave vector k^r at the emission point. By substituting Eqs. (A.3)-(A.4) into (A.7), one finds

$$K^2 = \frac{g_{tt}L_\gamma^2 + 2g_{t\varphi}L_\gamma E_\gamma + g_{\varphi\varphi}E_\gamma^2}{g_{rr}(g_{t\varphi}^2 - g_{tt}g_{\varphi\varphi})} + r_e^2 \frac{(E_\gamma g_{t\varphi} + L_\gamma g_{tt})^2}{(g_{t\varphi}^2 - g_{tt}g_{\varphi\varphi})^2}, \quad (\text{A.8})$$

in terms of the metric components and constants of motion. In addition, one can find a similar relation for K^2 by replacing Eq. (A.5) into (A.4) as follows

$$K^2 = \frac{g_{tt}L_\gamma^2 + 2g_{t\varphi}L_\gamma E_\gamma + g_{\varphi\varphi}E_\gamma^2}{g_{rr}(g_{t\varphi}^2 - g_{tt}g_{\varphi\varphi}) \cos^2 \alpha}. \quad (\text{A.9})$$

By equating the aforementioned equations for K^2 , we obtain the following relation for b_φ

$$(g_{tt}b_\varphi^2 + 2g_{t\varphi}b_\varphi + g_{\varphi\varphi})(g_{t\varphi}^2 - g_{tt}g_{\varphi\varphi}) \sin^2 \alpha - r_e^2 g_{rr} (g_{tt}b_\varphi + g_{t\varphi})^2 \cos^2 \alpha = 0, \quad (\text{A.10})$$

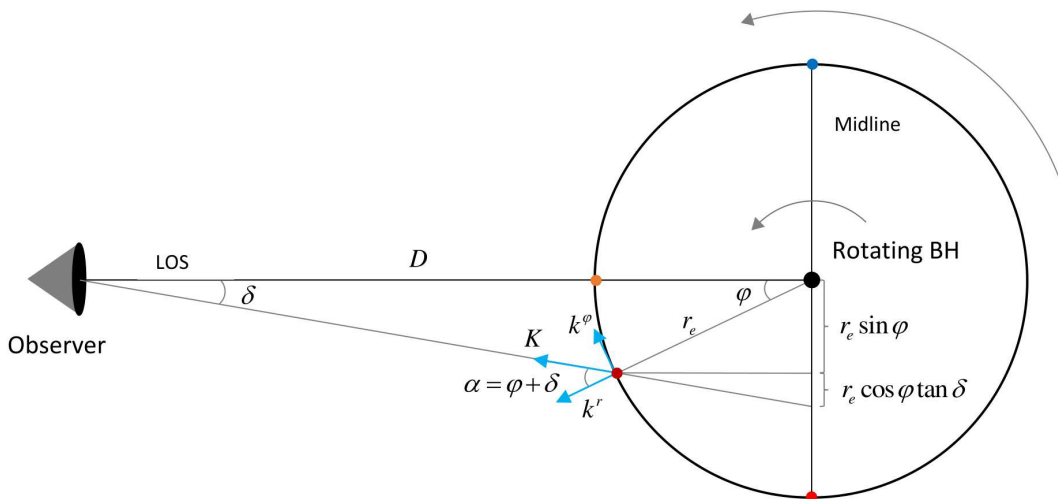


FIG. 2: The schematic illustration of a rotating black hole described by the line element (1) and a co-rotating photon source far enough from the black hole. This figure also shows the propagation direction K of the photons, and the relation between the unobservable azimuthal angle φ and the observable angular distance δ .

which gives the following solution for the α -dependent light bending parameter

$$b_\varphi = -\frac{g_{t\varphi}}{g_{tt}} - \frac{(g_{t\varphi}^2 - g_{tt}g_{\varphi\varphi}) \sin(\varphi + \delta)}{g_{tt}} \times \quad (\text{A.11})$$

$$\frac{1}{\sqrt{(g_{t\varphi}^2 - g_{tt}g_{\varphi\varphi}) \sin^2(\varphi + \delta) - r_e^2 g_{tt} g_{rr} \cos^2(\varphi + \delta)}},$$

that describes the light bending for a generic point of the circular orbit on the equatorial plane in the axially symmetric black hole spacetimes of the form (1).

On the other hand, we note that the angular distance δ is observable whereas the azimuthal angle φ is unobservable. In order to get rid of the unobservable parameter φ , we consider far-away emitters such that the geometrical configuration presented in Fig. 2 holds and the approximation $\alpha \approx \varphi + \delta$ is valid. This assumption is necessary to break the degeneracy of the mass-to-distance ratio and spin-to-distance ratio in the Kerr black hole spacetime. This allows us to extract a relation between δ and φ as follows (see Fig. 2)

$$D \sin \delta = r_e \sin(\varphi + \delta), \quad (\text{A.12})$$

where δ is observable only and D is the radial distance

between the black hole and the detector. Since it is not possible to locate the black hole's position on the sky with the help of observations, the rest of the parameters $\{D, r_e, \varphi\}$ are unknown. For the distant observers where $D \gg r_e$ and $\delta \rightarrow 0$, one finds that this relation reduces to

$$r_e \approx D \delta_m, \quad \text{for } \varphi_m = \pm \frac{\pi}{2}, \quad (\text{A.13})$$

$$r_e \approx \frac{D \delta_s}{\varphi_s}, \quad \text{for } \varphi_s \rightarrow 0, \quad (\text{A.14})$$

for the midline $\varphi = \varphi_m = \pm \pi/2$ and close to the LOS $\varphi = \varphi_s \rightarrow 0$, respectively. One can solve the relation (A.12) and express δ in terms of the rest of the parameters as follows

$$\delta = \arccos \left(\frac{D - r_e \cos \varphi}{\sqrt{D^2 + r_e^2 - 2Dr_e \cos \varphi}} \right), \quad (\text{A.15})$$

and note that we chose the acceptable solution of the angular distance since as φ decreases/increases, δ should decrease/increase in the same direction as well (see Fig. 2).

-
- [1] M. Momennia, P. Banerjee, A. Herrera-Aguilar and U. Nucamendi, *Schwarzschild black hole and redshift rapidity: A new approach towards measuring cosmic distances*, Eur. Phys. J. C 84, 583 (2024).
 [2] B. P. Abbott et al. (LIGO Scientific and Virgo Collaborations), *Observation of Gravitational Waves from a Binary Black Hole Merger*, Phys. Rev. Lett. 116, 061102 (2016).

- [3] K. Akiyama et al. (Event Horizon Telescope Collaboration), *First M87 Event Horizon Telescope Results. IV. Imaging the Central Supermassive Black Hole*, Astrophys. J. Lett. 875, L4 (2019).
 [4] K. Akiyama et al. (Event Horizon Telescope Collaboration), *First Sagittarius A* Event Horizon Telescope Results. VI. Testing the Black Hole Metric*, Astrophys. J. Lett. 930, L17 (2022).

- [5] A. Eckart and R. Genzel, *Observations of stellar proper motions near the Galactic Centre*, Nature (London) 383, 415 (1996).
- [6] A. M. Ghez, S. Salim, N. N. Weinberg, J. R. Lu, T. Do, J. K. Dunn, K. Matthews, M. R. Morris, S. Yelda, E. E. Becklin, T. Kremenek, M. Milosavljevic and J. Naiman, *Measuring Distance and Properties of the Milky Way's Central Supermassive Black Hole with Stellar Orbits*, Astrophys. J. 689, 1044 (2008).
- [7] S. Gillessen, F. Eisenhauer, S. Trippe, T. Alexander, R. Genzel, F. Martins and T. Ott, *Monitoring stellar orbits around the massive black hole in the galactic center*, Astrophys. J. 692, 1075 (2009).
- [8] M. R. Morris, L. Meyer and A. M. Ghez, *Galactic center research: manifestations of the central black hole*, Res. Astron. Astrophys. 12, 995 (2012).
- [9] S. Naoz, C. M. Will, E. Ramirez-Ruiz, A. Hees, A. M. Ghez and T. Do, *A Hidden Friend for the Galactic Center Black Hole, Sgr A**, Astrophys. J. Lett. 888, L8 (2020).
- [10] C. M. Will, S. Naoz, A. Hees, A. Tucker, E. Zhang, T. Do and A. Ghez, *Constraining a Companion of the Galactic Center Black Hole Sgr A**, Astrophys. J. 959, 58 (2023).
- [11] A. Herrera-Aguilar and U. Nucamendi, *Kerr black hole parameters in terms of the redshift/blueshift of photons emitted by geodesic particles*, Phys. Rev. D 92, 045024 (2015).
- [12] P. Banerjee, A. Herrera-Aguilar, M. Momennia and U. Nucamendi, *Mass and spin of Kerr black holes in terms of observational quantities: The dragging effect on the redshift*, Phys. Rev. D 105, 124037 (2022).
- [13] M. Momennia, A. Herrera-Aguilar and U. Nucamendi, *Kerr black hole in de Sitter spacetime and observational redshift: Toward a new method to measure the Hubble constant*, Phys. Rev. D 107, 104041 (2023).
- [14] J. R. Herrnstein, J. M. Moran, L. J. Greenhill and A. S. Trotter, *The Geometry of and Mass Accretion Rate through the Maser Accretion Disk in NGC 4258*, Astrophys. J. 629, 719 (2005).
- [15] A. L. Argon, L. J. Greenhill, M. J. Reid, J. M. Moran and E. M. L. Humphrey, *Toward a new geometric distance to the active Galaxy NGC 4258. I. VLBI monitoring of water maser emission*, Astrophys. J. 659, 1040 (2007).
- [16] E. M. L. Humphreys, M. J. Reid, J. M. Moran, L. J. Greenhill and A. L. Argon, *Toward a new geometric distance to the active galaxy NGC 4258. III. Final results and the Hubble constant*, Astrophys. J. 775, 13 (2013).
- [17] Q. M. Fu and X. Zhang, *Probing a polymerized black hole with the frequency shifts of photons*, Phys. Rev. D 107, 064019 (2023).
- [18] D. A. Martinez-Valera, M. Momennia and A. Herrera-Aguilar, *Observational redshift from general spherically symmetric black holes*, Eur. Phys. J. C 84, 288 (2024).
- [19] U. Nucamendi, A. Herrera-Aguilar, R. Lizardo-Castro and O. Lopez-Cruz, *Toward the gravitational redshift detection in NGC 4258 and the estimation of its black hole mass-to-distance ratio*, Astrophys. J. Lett. 917, L14 (2021).
- [20] A. Villalobos-Ramirez, O. Gallardo-Rivera, A. Herrera-Aguilar and U. Nucamendi, *A general relativistic estimation of the black hole mass-to-distance ratio at the core of TXS 2226-184*, Astron. Astrophys. 662, L9 (2022).
- [21] D. Villaraos, A. Herrera-Aguilar, U. Nucamendi, G. Gonzalez-Juarez and R. Lizardo-Castro, *A general relativistic mass-to-distance ratio for a set of megamaser AGN black holes*, MNRAS 517, 4213 (2022).
- [22] A. Gonzalez-Juarez, M. Momennia, A. Villalobos-Ramirez and A. Herrera-Aguilar, *Estimating the mass-to-distance ratio for a set of megamaser AGN black holes by employing a general relativistic method*, Astron. Astrophys. 689, A205 (2024).
- [23] A. Gonzalez-Juarez and A. Herrera-Aguilar, *IC 2560 and UGC 3193 megamaser AGN black hole mass estimations using general relativity*, [arXiv:2409.00772].
- [24] G. Morales-Herrera, P. Ortega-Ruiz, M. Momennia and A. Herrera-Aguilar, *Mass, charge, and distance to Reissner-Nordström black hole in terms of directly measurable quantities*, Eur. Phys. J. C 84, 525 (2024).
- [25] J. A. Braatz, M. J. Reid, E. M. L. Humphreys, C. Henkel, J. J. Condon and K. Y. Lo, *The megamaser cosmology project. II. The angular-diameter distance to UGC 3789*, Astrophys. J. 718, 657 (2010).
- [26] M. J. Reid, D. W. Pesce and A. G. Riess, *An improved distance to NGC 4258 and its implications for the Hubble constant*, Astrophys. J. Lett. 886, L27 (2019).
- [27] D. W. Pesce, J. A. Braatz, M. J. Reid, J. J. Condon, F. Gao, C. Henkel, C. Y. Kuo, K. Y. Lo and W. Zhao, *The Megamaser Cosmology Project. XI. A Geometric Distance to CGCG 074-064*, Astrophys. J. 890, 118 (2020).
- [28] C. Y. Kuo, J. A. Braatz, J. J. Condon, C. M. V. Impellizzeri, K. Y. Lo, I. Zaw, M. Schenker, C. Henkel, M. J. Reid and J. E. Greene, *The megamaser cosmology project. III. Accurate masses of seven supermassive black holes in active galaxies with circumnuclear megamaser disks*, Astrophys. J. 727, 20 (2011).
- [29] J. M. Bardeen and J. A. Petterson, *The Lense-Thirring effect and accretion disks around Kerr black holes*, Astrophys. J. Lett. 195, L65 (1975).
- [30] J. Darling, *How to detect inclined water maser disks (and possibly measure black hole masses)*, Astrophys. J. 100, 837 (2017).
- [31] J. M. Bardeen, W. H. Press and S. A. Teukolsky, *Rotating black holes: Locally nonrotating frames, energy extraction, and scalar synchrotron radiation*, Astrophys. J. 178, 347 (1972).
- [32] J. M. Moran, *The Black Hole Accretion Disk in NGC 4258: One of Nature's Most Beautiful Dynamical Systems*, ASP Conf. Ser. 395, 87 (2008).
- [33] M. J. Reid, J. A. Braatz, J. J. Condon, L. J. Greenhill, C. Henkel and K. Y. Lo, *The megamaser cosmology project. I. very long baseline interferometric observations of UGC 3789*, Astrophys. J. 695, 287 (2009).